Iranian Journal of Pharmaceutical Sciences
2025: 21 (1): 401-409
https://journals.sbmu.ac.ir/IJPS

Research Article

OPEN ACCESS

Pyrano[2,3-*d*]-pyrimidinedione Analogues Targeting Active Site of the H. Pylori Urease: Insights from Virtual Screening and ADMET Studies

Rakesh Amrutkar[a*], Anket Chhotu Pawar[a], Utkarsha Suhas Kulkarni[a], Ganesh B. Dabhade[b]

[a] *K K Wagh College of Pharmacy Nashik Maharashtra India.*
[b] *K. K. Wagh Institute of engineering Education and Research, Panchvati Nasik-422003, Maharashtra, India.*

Received: December 6, 2024 **Last Revision:** July 11, 2025 **Accepted:** July 21, 2025 **Available online:** September 23, 2025.

Abstract

To develop the views and application profiles of pyrano[2,3-d]pyrimidinedione, attempts have been made to account for drug/ligand or receptor/protein interactions by categorizing the suitable active site against the crystal structure of plant urease from jack bean (Canavalia ensiformis). The interaction was evaluated using the delta G value as the scoring function. The molecule with the most excellent negative delta G value is considered to have higher binding efficiency to the protein. The ligands AH4, AH8, and AH1 were shown to possess favorable negative values, indicating that these molecules have a greater affinity for the receptor's active site. The present research article also represents the Insilco ADMET and moderate biological activity of pyrano[2,3-d]pyrimidinedione. Some of the analogues exhibit hepatotoxicity and mutagenicity, as well as hERG K+ channel blocking activity. AH1 and AH2 inhibit cytochrome CYP1A2, affecting the metabolism of numerous xenobiotics. The present research work is beneficial for chemists working in the field of medicinal chemistry.

Keywords: ADMET; Molecular docking; pyrano [2,3-d]-pyrimidinedione; crystal structure of plant urease.

1. Introduction

The systematic study of six-membered nitrogen-containing heterocycles has consistently been of importance in the pharmaceutical and chemical fields, as they exhibit bioisosteric factors that are highly valuable for both theoretical and practical purposes. [1] Fused pyrano[2,3-*d*] pyrimidinedione is an unsaturated Nitro-heterocycle that consists of a pyran ring and a pyrimidine ring fused, with an oxygen atom at position eight and two nitrogen atoms at positions 1 and 3, respectively.[2] Organic compounds with these ring systems have diverse pharmacological properties, such as antiallergic [3], antihypertensive [4], cardiotonic [4], bronchodilator [5], antibronchial [6] antineoplastic [7, 8] antimalarial [9], anti-inflammatory [10] antiviral evaluation [11] antileishmanial [12,13] and antitubaercular [14]. The electron-donating and electron-withdrawing groups (such as 4–OCH_3, 4-Br, 4-Cl) and (4-NO_2) respectively, substituted on the phenyl ring which was substituted on the pyrano [2,3-*d*] pyrimidinedione structure exerts diverse control on its antibacterial action against various gram-positive and gram-negative bacteria, including *Bacillus cereus*, *Staphylococcus aureus*, *Escherichia*

*** Corresponding Author**:
Rakesh Amrutkar, K K Wagh College of Pharmacy Nashik Maharashtra India. E-mail: rakesh_2504@yahoo.co.in.

Cite this article as: Amrutkar R., Chhotu Pawar A., Suhas Kulkarni U., B. Dabhade G. Pyrano[2,3-d]-pyrimidinedione Analogues Targeting Active Site of the H. Pylori Urease: Insights from Virtual Screening and ADMET Studies. Iran. J. Pharm. Sci., 2025, 21 (1): 401-409.

DOI: https://doi.org/10.22037/ijps.v21i1.46925

coli, and *Pseudomonas aureus*. Substitution of heteroaryl, cyano, and amino groups on the pyrano[2,3-d]pyrimidine nucleus increases the penetration power of the product through the bacterial cell wall, thereby enhancing its efficacy as an antibacterial agent. [15-20]. Urease is a nickel-dependent metalloenzyme synthesized by plants, some bacteria, and fungi. [21].

The hydrolysis of urea into ammonia and carbon dioxide is a reaction catalyzed by urease. Although the amino acid sequences of plants and bacteria are closely linked, their biological activities differ. Additionally, plant ureases have insecticidal effects separate from their proteolytic activity [22]. Plant ureases are made up of a single-chain polypeptide in contrast to bacterial ureases, which consist of two or three polypeptides designated as α, β, and γ. Based on biochemical studies and the crystal structure of the *Klebsiella aerogenes* enzyme, the enzymatic mechanism proposes that urea binds to its carbonyl oxygen, which is bound to Ni1, and retains a water molecule in the Ni2 site [23, 24].

The stomach contains both acid and proteolytic enzymes, raising the longstanding question of how it digests food without damaging itself. For decades, scientists explored various explanations. One early hypothesis involved gastric urease, an enzyme thought to protect the stomach by neutralizing acid through the production of ammonia from urea, which diffuses from the blood. However, research stalled after it was discovered that gastric urease is not produced by mammalian cells. This changed with the discovery that *Helicobacter pylori*, a bacterium responsible for gastritis, peptic ulcers, and gastric cancer, actually produces the enzyme. Gastric urease enables *H. pylori* to survive in the highly acidic stomach environment, serving as a key biomarker for its presence. [25-37].

The primary objective of this work is to predict ADME, Tox profiles, pharmacokinetic properties, and adverse effects. Additionally, the interaction between protein/receptor and ligand/drug compounds of some novel pyrano [2,3-d]pyrimidinedione compounds has been reported.

2. Material and Methods

2.1. In Silico ADME screening

Swiss ADME freeware was used for the online *in silico* prediction of pharmacokinetic properties and drug likeness, including gastrointestinal absorption, blood-brain barrier penetration, skin permeability, synthetic associability, Lipinski, Ghose, and Veber rules, and bioavailability score [28,29]. The SMILES (Simplified Molecular Input Line Entry System) online [30] translator was used to build each compound. ChemSketch Freeware was used to create the two-dimensional structures, and the physicochemical parameters of the sketched molecules were calculated using the same program. [31]

2.2. Bioactivity Score Prediction

Pharmacological activity is a measure of a drug's advantageous impact on living organisms. The drug is intended to bind to a specific target, also referred to as a biological target. These targets are ubiquitous proteins, such as enzymes, ion channels, and receptors. The different parameters were taken into consideration for the calculation of bioactivity scores of the given molecules, such as binding to G-protein-coupled receptor (GPCR), ligand and nuclear receptor ligand, ion channel modulation, Kinase inhibition, protease inhibition, and enzyme activity inhibition with the help of Mol inspiration software [32] and predicted the pharmacological activity.

2.3. Toxicity prediction

The toxicity/adverse effects of the targeted compound were predicted using the PreTOX II [33] tool. The said tool predicts toxicity, including hepatotoxicity, cytotoxicity, carcinogenicity, mutagenicity, immunotoxicity, and adverse outcome pathways (Tox21). The potential biological properties of the selected compounds were also investigated through the PASS web server. The PASS tool enables us to explore the potential biological properties of compounds based on their chemical formula. It utilizes 2D molecular fragments, known as multilevel neighbors of atoms (MNA) descriptors, which suggest that the biological activity of a chemical compound is a function of its molecular structure. It gives the prediction score for biological properties on the ratio of 'probability to be active (Pa)' and 'probability to be inactive (Pi)'. A higher Pa means the biological property has a higher probability for a compound. Pred-HERG is an online tool for predicting QSAR models of hERG K+ channel blockage. [34, 35]. The accuracy of the prediction result is up to 60%. This method provides a straightforward

interpretation of the predicted activity, enabling the user to recommend structural modifications easily.

2.4. Molecular Docking

Molecular docking is used to estimate the interaction between a protein/receptor and a ligand/drug compound. The prediction of the drug-receptor interaction was performed using the SwissDock freeware available online [36].

2.5. Selection and Preparation of Protein/Receptor:

Initially, the protein/receptor (crystal structure of plant urease from jack bean (*Canavalia ensiformis* (**3LA4**) was downloaded from the protein data bank [37] (PDB), and then the receptor was prepared for docking by using Biovia Discovery Studio Visualizer [38] offline software and saved in PDB file format.

2.6. Selection, Preparation, and optimization of Ligand/drug:

The ligand/drug compound was prepared using the same software and saved as a mol2 file format. The Molecules Considered in the study are given in **Table 1**.

Table 1: Molecules Considered in the Study.

Compound Code	Structure	SMILES
AH1	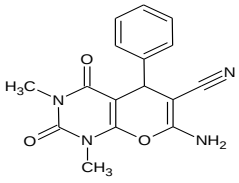	NC=1OC2=C(C(C=1C#N)c1ccccc1)C(=O)N(C)C(=O)N2C
AH2	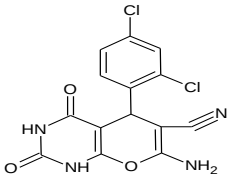	Clc1ccc(C2C(C#N)=C(N)OC=3NC(=O)NC(=O)C2=3)c(Cl)c1
AH3	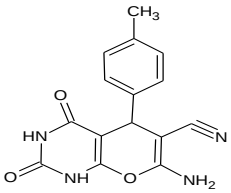	Cc1ccc(cc1)C1C(C#N)=C(N)OC=2NC(=O)NC(=O)C1=2
AH4	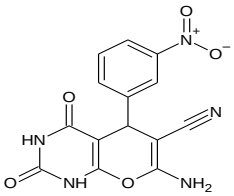	[O-][N+](=O)c1cccc(c1)C1C(C#N)=C(N)OC=2NC(=O)NC(=O)C1=2
AH5	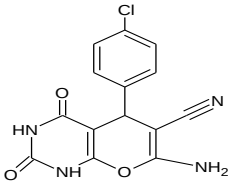	Clc1ccc(cc1)C1C(C#N)=C(N)OC=2NC(=O)NC(=O)C1=2
AH6	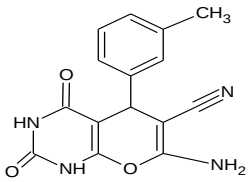	Cc1cccc(c1)C1C(C#N)=C(N)OC=2NC(=O)NC(=O)C1=2
AH7	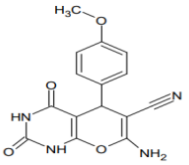	COc1ccc(cc1)C1C(C#N)=C(N)OC=2NC(=O)NC(=O)C1=2
AH8	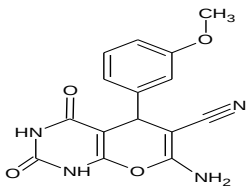	COc1cccc(c1)C1C(C#N)=C(N)OC=2NC(=O)NC(=O)C1=2
AH9	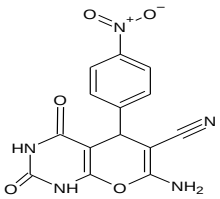	[O-] [N+] (=O) c1ccc (cc1) C1C (C#N)= C(N)OC =2NC (=O) NC (=O)C1=2
AH10	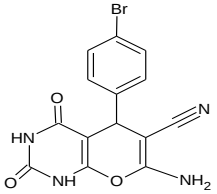	Brc1ccc(cc1)C1C(C#N)=C(N)OC=2NC(=O)NC(=O)C1=2

2.7. Molecular Docking:

Both the prepared ligand/drug and protein/receptor were uploaded to SwissDock for Molecular Docking. The results of docking were then analyzed using UCSF Chimera [39], a free, offline software.

3. Results and Discussion:

3.1. In Silico ADME screening

In this study, the Pharmacokinetic properties and drug-likeness prediction of all compounds were performed by SwissADME and are summarized in **Table 2**.

All molecules exhibit high GI absorption, except for molecule AH4, which also shows good skin permeation and inhibition of CYP1A2, a key enzyme in metabolism. Additionally, they are not substrates of P-glycoprotein, indicating good plasma concentration of the drug. P-glycoprotein, the most extensively studied ATP-binding cassette (ABC) transporter, functions as a biological barrier by extruding toxins and xenobiotics out of cells. Furthermore, LogP is a crucial component of Lipinski's Rule of 5. According to Lipinski's Rule of 5, an oral drug should have a LogP value <5, ideally between 1.35 and 1.8 for good oral and intestinal absorption.AH2, AH5, and AH10 contain logP values greater than 1.35, indicating good oral absorption.

3.2. Bioactivity Score Prediction

The bioactivity score is presented in **Table 3**. If the bioactivity score is greater than 0.0, the complex is considered active; if it is between −5.0 and 0.0, the complex is moderately active; and if the bioactivity score is less than −5.0, the complex is inactive.

Table 2: Pharmacokinetics and drug-likeness prediction of the compound.

Sr. No.	Compound Code	GI Absorption	BBB Penetration	P-gp	CYP1A2	LogP	LogS	Log $K_{p(Cm/s)}$	Bioavailability Score
1	AH1	High	NO	NO	NO	1.08	-3.13	-7.50	0.55
2	AH2	High	NO	NO	YES	1.96	-5.21	-7.11	0.55
3	AH3	High	NO	NO	NO	1.24	-4.40	-7.41	0.55
4	AH4	Low	NO	NO	NO	0.34	-3.38	-7.98	0.55
5	AH5	High	NO	NO	NO	1.45	-4.62	-7.34	0.55
6	AH6	High	NO	NO	NO	1.25	-4.40	-7.50	0.55
7	AH7	High	NO	NO	NO	0.91	-4.13	-7.11	0.55
8	AH8	High	NO	NO	NO	0.91	-4.13	-7.41	0.55
9	AH9	High	NO	NO	NO	0.33	-3.38	-7.98	0.55
10	AH10	High	NO	NO	YES	1.53	-4.83	-7.57	0.55

Table 3: Bioactivity score of the molecules

Sr. No.	Compound Code	Parameters of the Bioactivity score					
		GPCR ligand	Ion channel modulator	Kinase inhibitor	Nuclear receptor ligand	protease inhibitor	Enzyme inhibitor
1	**AH1**	-1.16	-1.32	-1.33	-0.82	-1.31	-0.74
2	**AH2**	-1.30	-1.37	-1.15	-0.97	-1.47	-0.81
3	**AH3**	-1.37	-1.48	-1.24	-0.93	-1.45	-0.81
4	**AH4**	-1.37	-1.36	-1.23	-0.92	-1.39	-0.83
5	**AH5**	-1.32	-1.41	-1.21	-0.92	-1.43	-0.79
6	**AH6**	-1.36	-1.49	-1.24	-0.92	-1.44	-0.81
7	**AH7**	-1.29	-1.42	-1.16	-0.86	-1.35	-0.78
8	**AH8**	-1.30	-1.43	-1.18	-0.85	-1.36	-0.77
9	**AH9**	-1.36	-1.34	-1.23	-0.91	-1.38	-0.81
10	**AH10**	-1.43	-1.49	-1.24	-1.02	-1.51	-0.83

3.3. Toxicity Prediction:

Toxicity studies of the molecules were conducted using the online toxicity prediction tool, i.e., ProTox-II. The analogues of pyrano[2,3-*d*]pyrimidinedione produce hepatotoxicity and carcinogenicity. From, all of the investigated compounds AH3, AH4, AH7, AH8, AH9, and AH10 are the hERG K^+ blockers. The details of toxicity studies for all molecules shown in **Tables 4**, and **Figure 1**.

The radar plot gives an efficient, multivariate visualization of predicted toxicity, enabling:

1. Quick identification of high-risk endpoints via radial expansion.
2. Quantitative ranking of compounds through enclosed area computation.
3. Guided experimental design by linking alerts to specific mechanistic assays.

The radar plot (**Figure 1**) shows substantially reduced predicted probabilities compared to the average library across nearly all endpoints, indicating a generally benign profile. The only moderate elevation (~40–50%) was observed for hepatotoxicity, ATAD5, and mitochondrial perturbation, suggesting potential mitochondrial dysfunction or DNA damage that warrants targeted in vitro confirmation using HepG2 cytotoxicity assays, JC-1 mitochondrial assays, or γH2AX DNA damage assays.

Table 4. Toxicity prediction of molecule.

Compound Code / Toxicity	AH 1	AH 2	AH 3	AH 4	AH 5	AH 6	AH 7	AH 8	AH 9	AH 10
Hepatotoxicity	Inactive	Active	Active	Active	Active	Active	Active	Active	Active	Active
Carcinogenicity	Inactive	Active	Active	Active	Active	Active	Active	Active	Active	Active
Mutagenicity	Inactive	Inactive	Inactive	Active	Inactive	Inactive	Inactive	Inactive	Inactive	Inactive
Immunotoxicity	Inactive	Inactive	Active	Active	Active	Inactive	Inactive	Inactive	Inactive	Inactive
K^+ Channel Blocker	Inactive	Inactive	Active	Active	Inactive	Inactive	Active	Active	Active	Active
Cytotoxicity	Inactive	Inactive	Inactive	Inactive	Inactive	Inactive	Inactive	Inactive	Inactive	Inactive
Aryl hydrocarbon Receptor (AhR)	Inactive	Inactive	Inactive	Inactive	Inactive	Inactive	Inactive	Inactive	Inactive	Inactive
Androgen Receptor (AR)	Inactive	Inactive	Inactive	Inactive	Inactive	Inactive	Inactive	Inactive	Inactive	Inactive
Androgen Receptor Ligand Binding Domain (AR-LBD)	Inactive	Inactive	Inactive	Inactive	Inactive	Inactive	Inactive	Inactive	Inactive	Inactive
Aromatase	Inactive	Inactive	Inactive	Inactive	Inactive	Inactive	Inactive	Inactive	Inactive	Inactive
Mitochondrial Membrane Potential (MMP)	Inactive	Inactive	Inactive	Inactive	Inactive	Inactive	Inactive	Inactive	Active	Inactive
Predicted LD 50 (mg/kg)	900	1600	2000	1600	1600	2800	4000	1600	1000	2000
Predicted Accuracy (%)	23%	23%	23.5%	23%	23%	22.9%	23%	23%	23.5%	24%

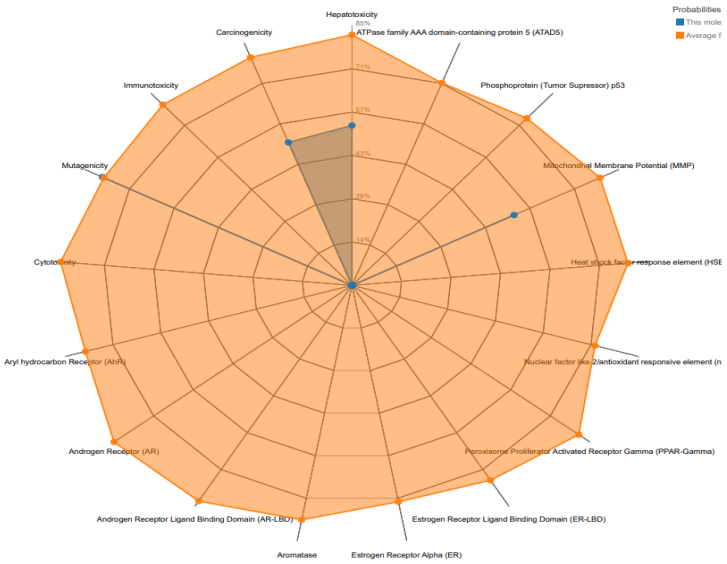

Figure 1. Toxicity Radar Chart of AH4 Molecule**.**

3.4. Molecular Docking

The results obtained from SwissDock were analyzed using UCSF Chimera (version 1.16). The binding affinity of a protein-ligand complex is correlated with the intermolecular interactions between these binding partners, solvent effects, and the dynamics of the complex. The most conventional method for estimating all these parameters simultaneously is to apply all-atom molecular dynamics (MD) simulations. However, to avoid the significant computational costs associated with these simulations, molecular docking employs scoring functions to provide a fast and approximate estimation of the binding affinity. Force-field-based, knowledge-based statistical functions are the three primary categories of scoring functions.

Along with this, the Empirical Scoring functions' efforts to estimate the binding affinity, which is directly related to the Gibbs energy of binding. Here, we consider the delta G value as the scoring function. The molecule with the greater negative delta G value is considered to have higher binding efficiency to the protein. The docking score was shown in **Table 5.**

Molecule (AH4)

The low **ΔG (kcal/mol)** of this ligand is **–7.53** kcal/mol against the binding site of the receptor (**Figure 2**).

Molecule (AH8)

The low ΔG (kcal/mol) of this ligand is – 7.36 kcal/mol against the binding site of the receptor (**Figure 3**).

Table 5. Molecular docking analysis.

Compound Code	Full Fitness (kcal/mol)	Estimated ΔG (kcal/mol)	Energy	InterFull	IntraFull	solvFull
AH1	-3768.97	-7.35	-4.29012	-37.9209	-72.8753	-4165.04
AH2	-3793.20	-7.08	0.24923	-31.6764	-94.8808	-4173.46
AH3	-3784.29	-7.19	-4.62636	-36.5056	-86.6111	-4166.96
AH4	-3663.47	-7.53	-4.62636	-43.6362	40.4542	-4167.35
AH5	-3784.92	-6.88	2.11202	-27.141	-86.7851	-4178.4
AH6	-3785.03	-7.34	-0.931395	-39.5363	-86.0002	-4166.43
AH7	-3783.53	-6.97	7.44354	-28.6489	-83.623	-4178.72
AH8	-3783.20	-7.36	3.33269	-40.4552	-83.7959	-4165.84
AH9	-3660.23	-6.84	114.827	-29.4217	40.6291	-4178.84
AH10	-3785.47	-7.00	1.43972	-27.6927	-86.7779	-4178.37

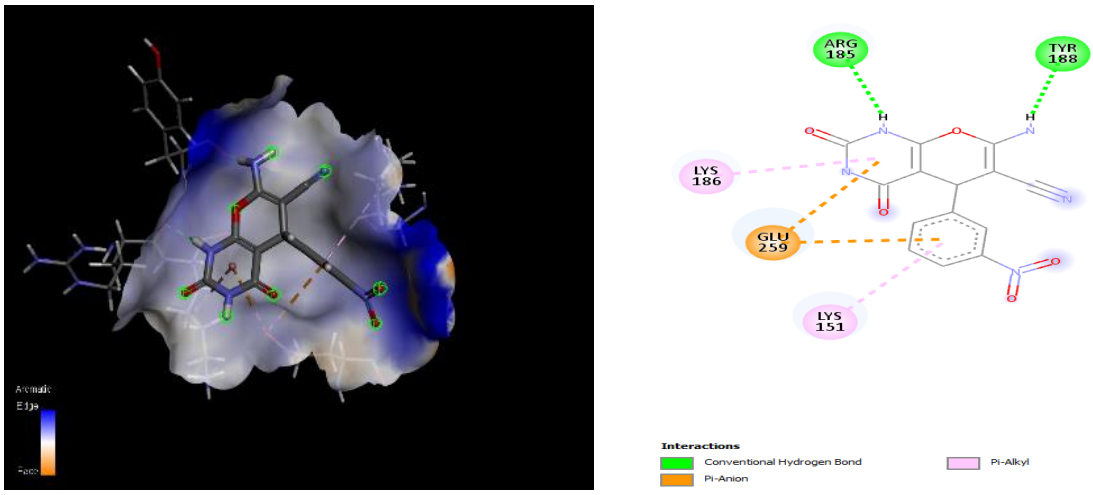

Figure 2. The Molecule (**AH4**) shows the hydrophobic bonding

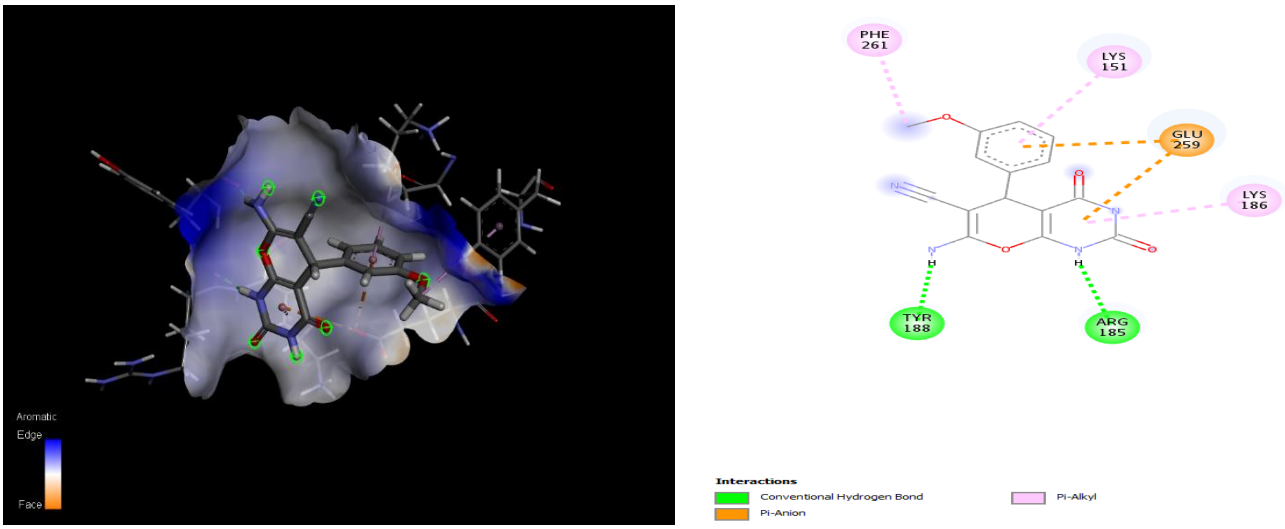

Figure 3. The Molecule (AH8) shows the hydrophobic bonding.

4. Conclusion

The data reported in this article may be helpful for medicinal chemists working in this area. Within this study, we predicted the biological activities and side effects of some 2,3-disubstituted pyranopyrimidinedione analogues. It has been confirmed that most of the compounds show good oral bioavailability and skin permeability, and they also exhibit high gastrointestinal absorption. Some of the analogues exhibit hepatotoxicity, mutagenicity, and block the hERG K+ channel. Compounds AH1 and AH2 inhibit cytochrome CYP1A2, which affects the metabolism of numerous xenobiotics. In the Present work, we have docked the ligand 2,3-disubstituted pyranopyrimidinedione analogues with proteins used as the targets of the crystal structures of the first plant urease from jack bean (3LA4) and *H. pylori* Urease**.** The interaction was evaluated based on the delta G value as the scoring function. The molecule with the greater negative ΔG value is considered to have higher binding efficiency to the protein. The ligands AH4, AH8, and AH1 were shown to possess a greater negative delta G value in Kcal/mol, i.e., these molecules have a higher affinity for the active site of the receptor.

Ethics Approval and Consent to Participate

No human or animal subjects were enrolled in the current study. The study's methodology was purely in vitro, so no ethical clearance was required for this study.

Consent for Publication

No patients, volunteers, or guardians of the children were involved in this study. The study's methodology was based on software.

Acknowledgment

The authors are grateful to the Management and Principal of K.K. Wagh College of Pharmacy, Nashik, for providing the necessary facilities.

Conflict of interest

The authors have declared that this text content has no conflicts of interest.

Data availability

All data generated or analyzed during this study are included in this published article.

Authors Contributions

Rakesh D Amrutkar : Conceptualization, Methodology, Writing – Review & Editing.
Anket C Pawar : Writing original draft
Utkarsha S Kulkarni : Data Analysis
Ganesh B Dabhade : Data Collection

Authors Orcid numbers:

Ganesh B. Dabhade: https://orcid.org/0000-0002-7743-2552

Rakesh D. Amrutkar: https://orcid.org/0000-0003-2262-1484

Utkarsha Kulkarni: https://orcid.org/0009-0009-9028-9584

Anket Pawar: https://orcid.org/0009-0008-7279-3034

Funding

No funding agency is involved in the present study.

Using artificial intelligence chatbots

There was no use of artificial intelligence in the making of this article.

References

1. Jampilek J. Heterocycles in medicinal chemistry. Molecules. (2019) 24(21): 3839 https://doi.org/10.3390/molecules24213839
2. Rezaeifard A, Bakherad M, Navidpour L, Abedi Bajestani M, Onagh G. Furo, Pyrano, and Pyrido [2, 3-d] Pyrimidines: A Comprehensive Review of Synthesis and Medicinal Applications. ChemistrySelect. (2024) 11; 9(10): e202302345. https://doi.org/10.1002/slct.202302345
3. Bhat AR, Dongre RS, Almalki FA, Berredjem M, Aissaoui M, Touzani R, Hadda TB, Akhter MS. Synthesis, biological activity and POM/DFT/docking analyses of annulated pyrano [2, 3-d] pyrimidine derivatives: Identification of antibacterial and antitumor pharmacophore sites. Bioorganic Chemistry. (2021) 106: 104480. http://dx.doi.org/10.1016/j.bioorg.2020.104480
4. Bennett LR, Blankley CJ, Fleming RW, Smith RD, Tessman DK. Antihypertensive activity of 6-arylpyrido [2, 3-d] pyrimidin-7-amine derivatives. Journal of medicinal chemistry. (1981) 24(4): 382-9. 10.1021/jm00136a006
5. Heber D, Heers C, Ravens U. Positive inotropic activity of 5-amino-6-cyano-1,3-dimethyl-1,2,3,4-tetrahydropyrido[2,3-d]pyrimidine-2,4-dione in cardiac muscle from guinea-pig and man. Part 6: Compounds with positive inotropic activity. Pharmazie. (1993); 48(7): 537–41 PMID: 7692456.
6. Coates WJ. Pyrimidopyrimidine Derivatives. Eur Pat 351058. ChemAbstr. (1990) 113: 40711. [Google Scholar]
7. Abd El-Sattar NEA, El-Adl K, El-Hashash MA, Salama SA, Elhady MM. Design, synthesis, molecular docking and in silico ADMET profile of pyrano[2,3-d] pyrimidine derivatives as antimicrobial and anticancer agents. BioorgChem [Internet]. (2021); 115:105186. Available from: http://dx.doi.org/10.1016/j.bioorg.2021.105186
8. Zeinab Hussain, Magdy A. Ibrahim, Noha M. Hassanin, Al-Shimaa Badran, Synthetic approaches for novel annulated pyrido[2,3-d]pyrimidines: Design, Structural Characterization, Fukui functions, DFT Calculations, Molecular docking and Anticancer efficiency ,Journal of Molecular Structure, (2024) ;1318, Part 1:139335. https://doi.org/10.1016/j.molstruc.2024.139335
9. Davoll J, Clarke J, Elslager EF. Antimalarial substances. 26. Folate antagonists. 4. Antimalarial and antimetabolite effects of 2, 4-diamino-6-[(benzyl) amino] pyrido [2, 3-d] pyrimidines. Journal of Medicinal Chemistry. (1972) 15(8): 837-9. 10.1021/jm00278a009
10. H ur Rashid H, Martines MA, Duarte AP, Jorge J, Rasool S, Muhammad R, Ahmad N, Umar MN. Research developments in the syntheses, anti-inflammatory activities and structure–activity relationships of pyrimidines. RSC advances. (2021) 11 (11): 6060-98. DOI https://doi.org/10.1039/D0RA10657G
11. Shamroukh AH, Zaki ME, Morsy EM, Abdel-Motti FM, Abdel-Megeid FM. Synthesis of pyrazolo [4′, 3′: 5, 6] pyrano [2, 3-d] pyrimidine derivatives for antiviral evaluation. Archiv der Pharmazie: An International Journal Pharmaceutical and Medicinal Chemistry. (2007); 340(5): 236-43. 10.1002/ardp.200700005
12. Sabet R, Hatam G, Emami L, Ataollahi E, Zare F, Zamani L, Kazemi B, Jahromi MM, Sadeghian S, Khabnadideh S. Pyrazole derivatives as antileishmanial agents: Biological evaluation, molecular docking study, DFT analysis and ADME prediction. Heliyon. (2024); 19:10(23): e40444. https://doi.org/10.1016/j.heliyon.2024.e40444
13. Anu Agarwal, Ramesh, Ashutosh, Neena Goyal, Prem M.S. Chauhan, Suman Gupta, Dihydropyrido[2,3-d]pyrimidines as a new class of antileishmanial agents, Bioorganic & Medicinal Chemistry, (2005); 13(24): 6678-6684. https://doi.org/10.1016/j.bmc.2005.07.043
14. Kamdar NR, Haveliwala DD, Mistry PT, Patel SK. Design , synthesis and in vitro evaluation of antitubercular and antimicrobial activity of some novel pyranopyrimidines. European Journal of Medicinal Chemistry.(2010); 45(11) : 5056–63 http://dx.doi.org/10.1016/j.ejmech.2010.08.014
15. Broom AD, Shim JL, Anderson GL. Pyrido [2, 3-d] pyrimidines. IV. Synthetic studies leading to various oxopyrido [2, 3-d] pyrimidines. The Journal of organic chemistry. (1976) 41(7):1095-9. https://doi.org/10.1021/jo00869a003
16. Organic Chemistry, By Robert Thornton Morrison and Robert Neilson Boyd, Pearson Education , New Delhi, 6th Edition page 262-265.
17. Bararjanian M, Balalaie S, Movassag B, Amani AM. One-pot synthesis of pyrano[2,3-d]pyrimidinone

derivatives catalyzed by L-proline in aqueous media. J Iran ChemSoc [Internet]. (2009) 6(2):436–42. http://dx.doi.org/10.1007/bf03245854.
18. Sakuma Y, Hasegawa M, Kataoka K, Hoshina K, Yamazaki N, Kadota T, Yamaguchi H. WO 91/05785 PCT Int Appl 1989 Chem Abstr (1991) 115: 71646.
19. Broom AD, Shim JL, Anderson GL. Pyrido[2, 3-d]pyrimidines. IV. Synthetic studies leading to various oxopyrido [2, 3-d] pyrimidines. J Org Chem. (1976) 41: 1095. *doi:* 10.1021/jo00869a003.
20. Prasanth GK, Divya LM, Sadasivan C. Bisphenol-A can bind to human glucocorticoid receptor as an agonist: an in silico study. J Appl Toxicol (2010) 30(8):769–74. http://dx.doi.org/10.1002/jat.1570.
21. David Y. Graham, Muhammad Miftahussurur, Helicobacter pylori urease for diagnosis of Helicobacter pylori infection: A mini review, Journal of Advanced Research (2018); 13:51-57 https://doi.org/10.1016/j.jare.2018.01.006
22. Dunn BE, Phadnis SH. Structure, function and localization of Helicobacter pylori urease. Yale J. Biol Med. (1998); 71(2): 63-73.
23. Omar Hashem, Sumera Zaib, Seyed-Omar Zaraei, Hira Javed, Reena A. Kedia, Hanan S. Anbar, Imtiaz Khan, Anil Ravi, Mohammed I. El-Gamal, Ghalia Khoder, Design and discovery of urease and Helicobacter pylori inhibitors based on benzofuran/benzothiophene-sulfonate and sulfamate scaffolds for the treatment of ureolytic bacterial infections, International Journal of Biological Macromolecules, (2024) ; 271(1):132502. https://doi.org/10.1016/j.ijbiomac.2024.132502
24. Silva LM, Salgado AM, Coelho MA, Vermelho AB, Couri S. Urease activity. Methods to determine enzymatic activity. (2013); 22: 292-319. 10.2174/97816080530011130101
25. Ziarani GM, Faramarzi S, Asadi S, Badiei A, Bazl R, Amanlou M. Three-component synthesis of pyrano[2,3-d]-pyrimidine dione derivatives facilitated by sulfonic acid nanoporous silica (SBA-Pr-SO3H) and their docking and urease inhibitory activity. Daru [Internet]. (2013) 21(1):3. http://dx.doi.org/10.1186/2008-2231-21-3
26. Anuradha Balasubramanian, Karthe Ponnuraj, Crystal structure of the first plant urease from jack bean: 83 years of journey from its first crystal to molecular structure J MolBiol. (2010) 400(3):274-83. doi: 10.1016/j.jmb.2010.05.009.
27. Ureases: Historical aspects, catalytic, and non-catalytic properties – A review Karine Kappaun, Angela Regina Piovesan, Celia Regina arlini, and Rodrigo Ligabue- Braunc, Journal of advance research (2018) 13: 3–17.
28. Leong IUS, Stuckey A, Lai D, Skinner JR, Love DR. Assessment of the predictive accuracy of five in silico prediction tools, alone or in combination, and two metaservers to classify long QT syndrome gene mutations. BMC Med Genet. (2015) 16(1): 34. http://dx.doi.org/10.1186/s12881-015-0176-z
29. Lipinski CA, Lombardo F, Dominy BW, Feeney PJ. Experimental and computational approaches to estimate solubility and permeability in drug discovery and development settings 1PII, Advanced Drug Delivery Reviews 23 (1997) 3–25. 1. Adv Drug Deliv Rev [Internet]. (2001) 46(1–3):3–26. http://dx.doi.org/10.1016/s0169-409x(00)00129-0
30. SwissADME [Internet]. Swissadme.ch. [cited 2023 Jan 29]. Available from: http://www.swissadme.ch/
31. Free chemical drawing software for students [Internet]. ACD/Labs. (2022) [cited 2023 Jan 29]. Available from: https://www.acdlabs.com/resources/free-chemistry-software-apps/chemsketch-freeware/
32. Mol inspiration cheminformatics. Choice (Middletown) [Internet]. (2006) [cited 2023 Jan 29] ; 43(11):43-6538-43–6538. Available from: https://www.molinspiration.com/
33. ProTox-II - prediction of TOXicity of chemicals [Internet]. Charite.de. [cited 2023 Jan 29]. Available from: https://tox-new.charite.de/protox_II/index.php?site=compound_input
34. LabMol [Internet]. Com.br. [cited 2023 Jan 29]. Available from: http://predherg.labmol.com.br/
35. Lin JH, Yamazaki M. Role of P-glycoprotein in pharmacokinetics: clinical implications: Clinical implications. ClinPharmacokinet [Internet]. (2003) 42(1):59–98. Available from: http://dx.doi.org/10.2165/00003088-200342010-00003.
36. Grosdidier, A. (n.d.). SwissDock. Swissdock.Ch. Retrieved December 24, 2022, from http://www.swissdock.ch/
37. RCSB Protein Data Bank. (n.d.). RCSB PDB: Homepage. Rcsb.org. Retrieved December 24, 2022, from https://www.rcsb.org/
38. Visualization. (n.d.). 3ds.com. Retrieved December 24, 2022, from https://www.3ds.com/products-services/biovia/products/molecular-modeling-simulation/biovia-discovery-studio/visualization/
39. Download UCSF Chimera. (n.d.). Ucsf.edu. Retrieved December 24, 2022, from https://www.cgl.ucsf.edu/chimera/download.html